Asian Journal of Electrical Sciences
ISSN: 2249-6297 (P) Vol.5 No.2, 2016, pp.33-43

DOI: https://doi.org/10.51983/ajes-2016.5.2.1979

Optimization of Synchronous Non-Isolated Bidirectional DC-DC Switching Power Converter

N.M.Mahesh Gowda[1] and S.S. Parthasarathy[2]
[1] Assistant Professor, Dept. of Electronics and Communication Engineering,
[2]Professor, Dept. of Electrical and Electronics Engineering,
PES College of Engineering, Mandya, Karnataka, India.
E-mail: nm_maheshg@yahoo.co.in

Abstract **- This paper presents a high-efficiency non-isolated synchronous bidirectional DC-DC switching power converter. The circuit is made to operate in Synchronous Discontinuous Conduction Mode (SDCM)/Forced Continuous Conduction Mode (FCCM) of operation for minimum inductor value, to reduce the size, weight and cost of the converter. A snubber capacitor is used across the switch to minimize turn-off loss. The power dissipation through snubber capacitor and inductor is minimized by proper selection of their value, which improves the efficiency of the converter. Complementary gate signals are used to control the ON and OFF of main and auxiliary switch. By use of SDCM of operation, complementary gate signals control scheme and snubber capacitor, turn-on loss and parasitic ringing effect is minimized. State space averaging method is used to obtain control-to-current transfer function module. Using the transfer function module, Proportional Integral Derivative (PID) controller is tuned using PID tuner software, available in MATLAB simulink control design block to regulate load voltage and load current for change in inductor reference current (*I**), change in load resistance and change in input voltage. The modules are verified using MATLAB simulink simulator.**

Keywords**: SDCM, buck, boost, bidirectional, non-isolated, PI controller, MATLAB, simulink.**

I. INTRODUCTION

Switching DC-DC converters are power electronic circuits which transfer one level of electrical voltage into another level by switching action. These converters are implemented in numerous fields like Uninterrupted Power Supplies (UPS), telecommunication purpose, DC machine drives, aerodynamics, hybrid electric and fuel cell vehicles [1][2], renewable energy system etc. The analyses, control and stabilization of switching power converters are the important circumstance that requires to be taken into account. Many regulate types are used for control of switching DC-DC converters and the simple, straightforward and low cost control framework is in require for all industrial and large capability uses. Voltage-mode regulate and current-mode regulate are two commonly used regulate schemes to regulate the output voltage and current of DC-DC converters [3].

Feedback loop type automatically maintains a precise output voltage and current regardless of variation in load conditions, input voltage and current. Currently, there exist more than one different control approach, for example PI control method [2], PID controller [4][5], state space averaging type regulate [6], pulse width modulation and PID control technique [7], sliding mode regulate [8], fuzzy logic regulate[9][4], etc. Each regulate type has its own advantages and disadvantages, and its efficient find out by the use where it is applied.

In the proposed research work, control-to-current transfer function module is derived using state space averaging method. Using derived transfer function module, PID values are tuned by using PID tuner software available in MATLAB simulink control design block, for unit step input, to achieve good transient response. The obtained P, I and D values are further fine tuned by trial and error method with feedback PID controller of system models (simulink bidirectional module) for good stable operation. The fine tuned PID gains are tested with unit step input, which gives better transient response. The fine tuned P, I and D values are considered as optimal unique PID gains for bidirectional mode of operation. The module is tested for different test cases like change in inductor reference current (*I**), change in load resistance and change in input voltage. For each case, output voltage (V_2), output current (I_2), load power (P_o), peak inductor current (I_{peak}), minimum inductor current (I_{min}), average inductor current (I_L), ripple current of inductor (ΔI_L), efficiency (η) and duty cycle (D) are measured. From the obtained results it is noted that the theoretical and simulation measurement are comparable. The feedback controller works as expected.

II. PROPOSED SYSTEM

A non-isolated synchronous bidirectional switching DC-DC power converter technology is to combine a buck and boost mode of operation. Complementary gate signal control scheme is used to control the ON and OFF of transistor switches. The converter is implemented to operate in SDCM such that the inductor size, cost, converter size and weight can be reduced. The SDCM operation introduces turn-off loss. This is one of the drawback of the inductor size reduction. The snubber capacitor added across the transistor switch is to reduce turn off loss. Snubber capacitor requires certain amount of energy stored in the inductor to discharge

the capacitor energy before device is turned on. The main advantage of the SDCM of operation is minimum turn-on loss due to complementary gating signal control scheme and by use of snubber capacitor, thus low diode reverse recovery loss. Thus both soft switching turn-on and -off are obtained. The optimization of size, cost and efficiency can be done by proper selecting of circuit parameters like snubber capacitor, inductor, switching device, switching frequency and load resistor.

.

Fig.1 shows the circuit topology, where V_H and V_L are the voltage source at high side (V_1) and low side (V_2) voltage respectively, R_1 is the internal resistance of V_H, R_2 is the load resistance at low voltage side, C_H and C_L are the input and output capacitors to smooth the load current. Q_1 and Q_2 are MOSFETs, acts as switches with body diode D_1 and D_2 respectively. C_1 and C_2 are snubber capacitors. L is the inductor with parasitic resistance R_{LP}. In buck mode of operation the inductor average current is positive and in boost mode it is negative.

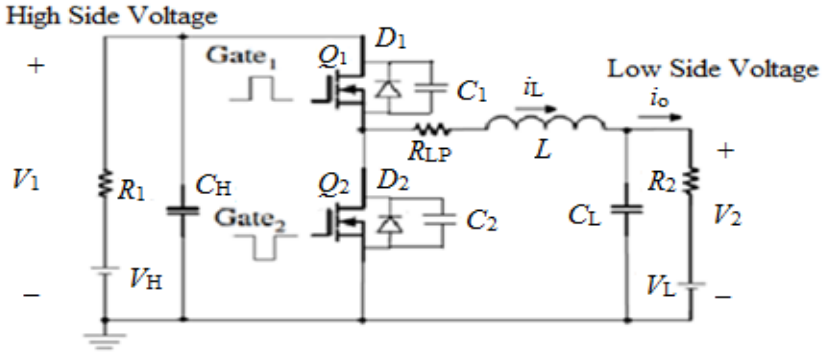

Fig.1 Circuit topology

III. POWER STAGE MODELING

The circuit shown in Fig 1 is used as buck and boost mode of operation. In these modes of operation there are two intervals, turn on and turn off as shown in Fig 2.

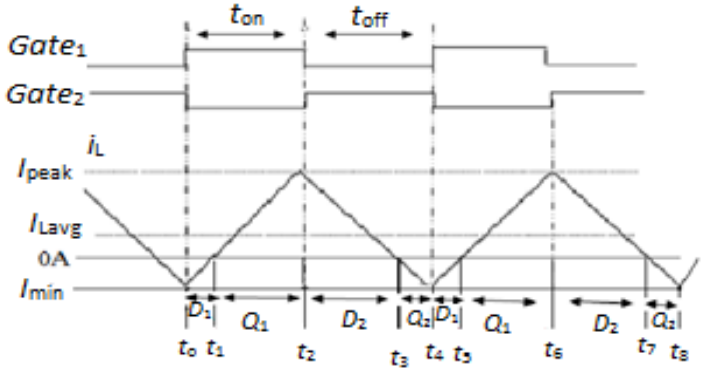

Fig.2 Ripple current of inductor with on and off intervals.

At time t_1, Q_1 is on, the inductor current is positive, moving towards V_L and reach its peak value in time t_2. At time t_2, Q_2 is on and Q_1 is off, during this time, diode D_2 carries the freewheeling current. With the voltage V_2 against the inductor, the current reduces until it passes through zero and changes its direction. At this time t_3, the current will flows through the auxiliary switch Q_2. Now the diode D_2 turn off naturally without having reverse recovery loss. At time t_4, Q_1 is on and Q_2 is off. During this time, diode D_1 will carry the inductor negative current. The voltage difference between V_1 and V_2 will appear across the inductor L, and the inductor current will increase towards positive direction and reaches zero in time t_5 and switch over to positive direction, and the main switch Q_1 takes the current. The cycle repeats. I_{peak}, I_{min} and ΔI_L is given in equations (1 – 3)

$$I_{peak} = I_L + \Delta I_L \quad (1)$$

$$I_{min} = I_L - \Delta I_L \quad (2)$$

$$\Delta I_L = \frac{1}{2} . \frac{V_{in} - V_{out}}{L} . \frac{V_{out}}{V_{in}} . T_s \quad (3)$$

Where V_{in}=V_1, V_{out}=V_2 and T_s is the switching period.

Using state space averaging method, average inductor current (I_L), high side voltage (V_1), low side voltage (V_2) and control to current transfer function is derived and is given in equations (4-7).

$$I_L = \frac{DV_H - V_L}{R_1 D^2 + R_2 + R_P} \quad (4)$$

$$V_1 = \frac{V_H(R_2+R_P)+DR_1V_L}{R_1D^2+R_2+R_P} \quad (5)$$

$$V_2 = \frac{D(V_H R_2 + DR_1V_L)+R_PV_L}{R_1D^2+R_2+R_P} \quad (6)$$

$$G_{id} = \frac{\hat{i_L}}{\hat{d}} = \frac{\left(s+\frac{1}{C_H.R_1}\right).\left(s+\frac{1}{C_L.R_2}\right).\frac{V_1}{L} - \frac{D.I_L}{C_H.L}.(s+\frac{1}{C_L.R_2})}{\left(s+\frac{R_P}{L}\right).\left(s+\frac{1}{C_H.R_1}\right).\left(s+\frac{1}{C_LR_2}\right)+\frac{D^2.(s+\frac{1}{C_L.R_2})}{L.C_H}+\frac{(s+\frac{1}{C_H.R_1})}{L.C_L}} \quad (7)$$

where D = Duty cycle, $R_P = R_{dson} + R_{LP}$, R_{dson} = turn-on resistance of MOSFET.

IV. CURRENT FLOW DIRECTION

Current flow direction in bidirectional DC-DC converter is shown in Fig.3. D_o is called zero current duty cycle, because at this value of duty cycle inductor average current (I_L) is zero and it is given in equation (8). D is the control duty cycle and given in equation (9)

$$D_o = \frac{V_L}{V_H} \quad (8)$$

$$D = \frac{V_H - \sqrt{V_H^2 - 4(I_L.R_1)(I_L.R_2 + I_L.R_P + V_L)}}{2(I_L.R_1)}, \quad (9)$$

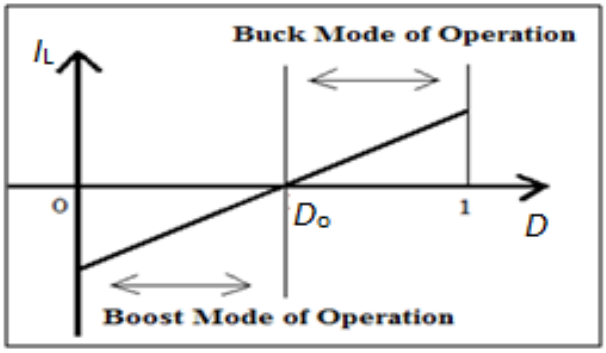

Fig. 3 Direction of current flow

In buck mode of operation, D is greater than D_o and the I_L is positive. In boost mode of operation, D is less than D_o and I_L is negative. The minimum and maximum range of I_L and D for different test parameters is given in Table 1. In duplex buck mode, when I_L falls below 0.1A, duty cycle also drops and further falling I_L towards non-positive value, duty cycle D becomes smaller than D_o and the system moves into boost mode. In duplex boost mode of operation, when I_L moves towards zero, D begin to divert towards D_o and further moving I_L above zero, D becomes larger than D_o and the system enters into buck mode of operation.

TABLE 1 DUTY CYCLE AND AVERAGE INDUCTOR CURRENT LIMIT FOR DIFFERENT RANGE OF PARAMETERS.

Mode of operation	V_H [V]	V_L [V]	R_1 [mΩ]	R_2[Ω]	R_p [mΩ]	D_o [%]	I_L [A]	D [%]
Bidirectional Buck Mode	250	110	10	2	71	44	≤ 0.1	≤ 44.08
						44	67.2	99.93
	250	110	10	1	71	44	≤ 0.1	≤ 44.04
						44	129.5	99.99
	260	110	10	2	71	42.30	≤ 0.1	≤ 42.38
						42.30	72	99.93
Bidirectional Boost Mode	250	110	10	2	71	44	≤ - 0.1	≥ 43.91
						44	≥ - 51.9	≤ 1
	250	110	10	1	71	44	≤ - 0.1	≥ 43.95
						44	≥ - 100.3	≤ 1.03
	260	110	10	2	71	42.30	≤ - 0.1	≥ 42.22
						42.30	≥ - 51.8	≤ 1.04

V. EFFICIENCY MEASUREMENT

Power loss in DC-DC converter exist through the MOSFET conduction, diode conduction, MOSFET switching, inductor and through snubber capacitor. The efficiency of the converter is given in equation (7)

$$\eta = \left(\frac{P_o}{P_o+P_{sw-con}+P_{d-con}+P_{sw1}+P_{sw2}+P_L+P_{s-cap}}\right).100\%, \quad (10)$$

where P_o = output power, $P_{sw\text{-}con}$ = switch conduction loss, $P_{d\text{-}con}$ = diode conduction loss, P_{sw1} = loss during switch transition, P_{sw2} = loss during discharging of the drain to source capacitor of the MOSFET during turn on, P_L = inductor loss and $P_{s\text{-}cap}$ = snubber capacitor loss.

VI. PID CONTROLLER

Proportional-Integral (PI) controller is used as a feedback controller with inductor current as a feedback reference as shown in Fig.4.

Using transfer function of equation (4), *P*, *I* and *D* values are obtained by tuning PID tuner software available in MATLAB simulink control design block as shown in block diagram of Fig.5. Optimal unique *P*, *I* and *D* gains are investigated by fine tuning around the tuned PID values by trial and error method with feedback PID controller of system model (simulink module of duplex DC-DC converter) for good stable performance. The identified unique PID gains are 0.000123, 60 and 0 respectively. Since *D*=0, PI controller is considered as a feedback controller in bidirectional DC-DC topology module instead of PID controller. The discovered optimal unique PID gains are tested with unit step input, which gives better transient response as shown in Fig 6, for case1 test parameter and the same is performed for other cases. The corresponding transient response parameters for three different test cases are tabulated in Table 2.

.

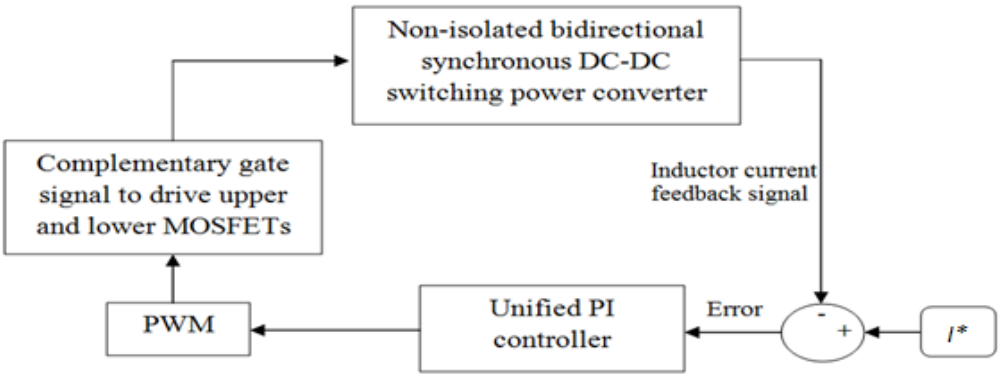

Fig.4 Block diagram of feedback controller in duplex DC-DC converter.

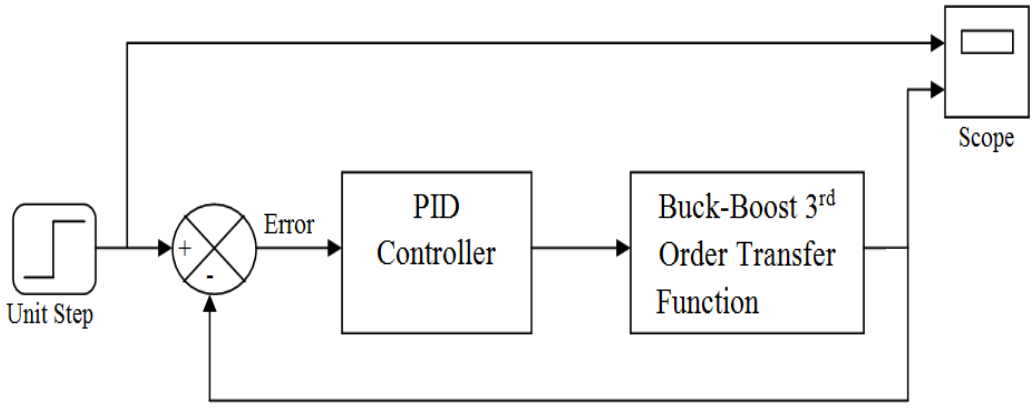

Fig.5 PID Tuner block diagram.

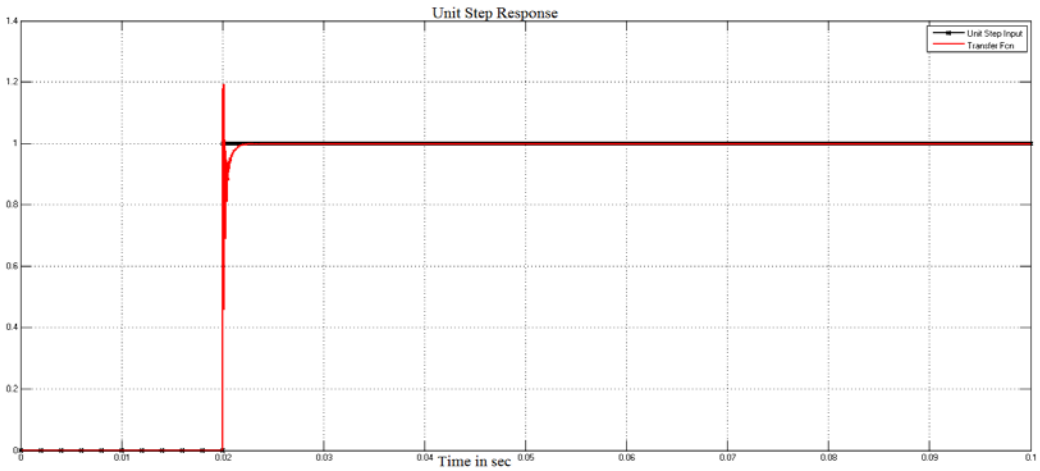

(a)

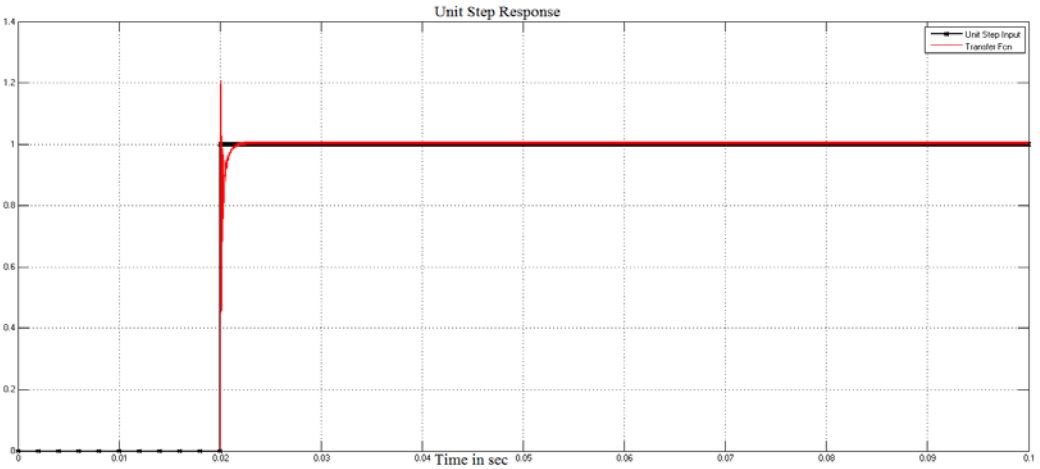

(b)

Fig.6 Unit step response of bidirectional DC-DC converter parameters for case1 (a) Buck mode (b) Boost mode.

TABLE 2 TRANSIENT RESPONSE PARAMETERS FOR BUCK-BOOST MODE OF OPERATION FOR STEP INPUT CONSIDERING UNIQUE PID GAIN.

Case	V_L [V]	V_H [V]	R_1 [mΩ]	R_2 [Ω]	I^* [A]	t_r [ms]	t_s [ms]	OS [%]	e_{ss} [%]
1	110	250	10	2	30	0.0331	1.6	19.27	-0.03
	110	250	10	2	-20	0.0329	1.5	20.62	0.1
2	110	250	10	1	30	0.0329	1	21.24	-0.06
	110	250	10	1	-20	0.0328	0.8	22.46	0.15
3	110	260	10	2	30	0.0322	1.6	20.85	-0.03
	110	260	10	2	-20	0.032	1.4	22.12	0.1

From Table 2, it is observed that the system has small steady state error, reach steady state within 1.6ms and moderate percentage overshoot.

.

VII. RESULTS

Circuit parameters value is given in Table 3.

TABLE 3 CIRCUIT PARAMETERS FOR BIDIRECTIONAL DC-DC CONVERTER.

V_H [V]	V_L [V]	R_1 [mΩ]	R_2 [Ω]	C_H=C_L [μF]	L [μH]	f_{SW} [kHz]	R_{dson} [mΩ]	R_{LP} [mΩ]	C_1=C_2 [nF]
250	110	10	2	150	10	50	35	36	15

Case 1: Change in inductor reference current

Here the inductor reference current changes from 30 A to -20 A. A simulation result is shown in Fig 7. In the beginning stage, load current I_2 and load voltage V_2 takes around 3ms to reach steady state value of 30±0.5 A and 170±1 V respectively. The inductor current i_L is averaged at 29.42 A. With change in I^*, I_2 and V_2 decreases smoothly from 30±0.5 A to -20±0.5 A and from 170±1 V to 70±1 V respectively and they takes around 2ms to reach steady state value. The inductor current averaged at -19.48 A. Variation of efficiency at different levels of load current is shown in Fig 8.

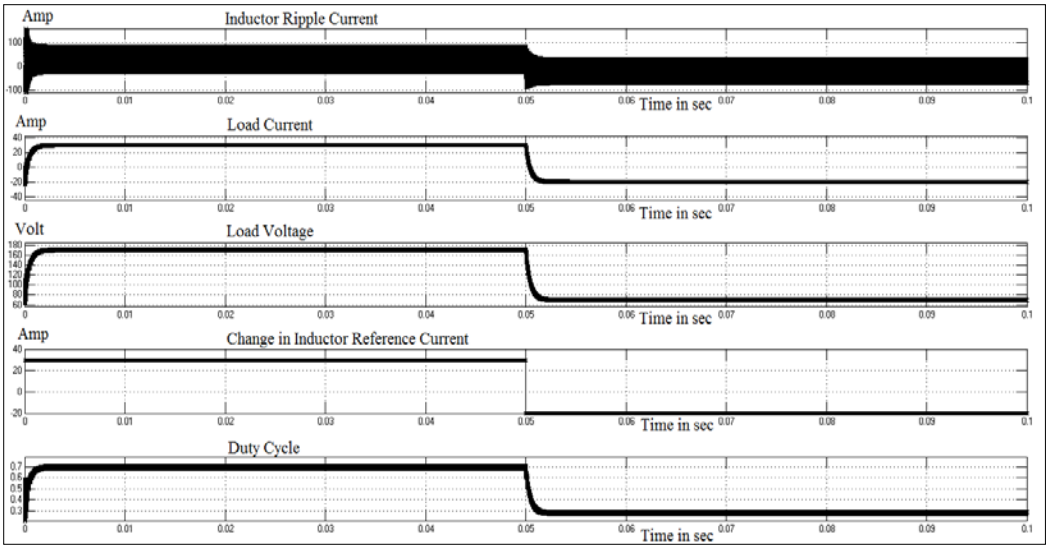

Fig.7 Simulation results for change in inductor reference current.

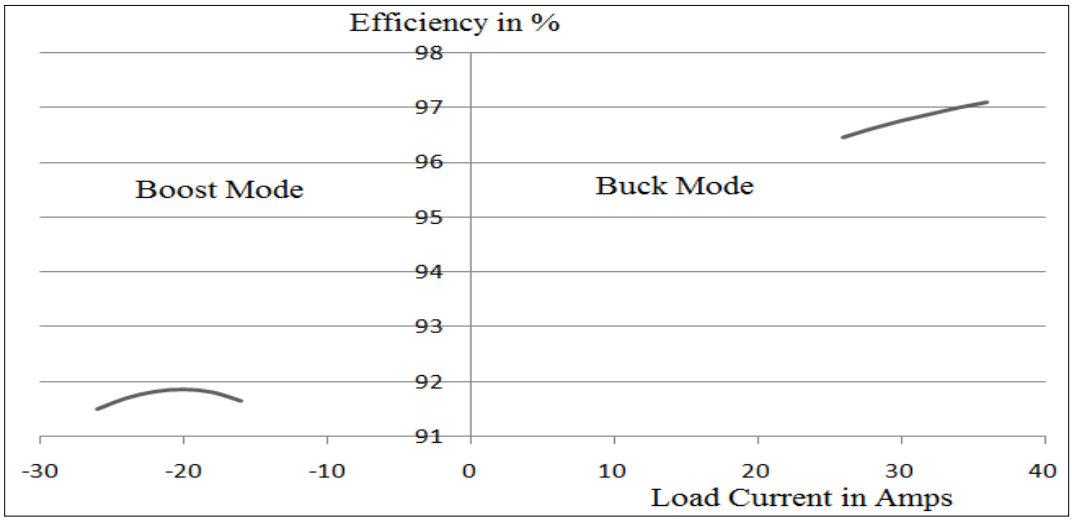

Fig.8 Load current v/s efficiency.

Case 2: Change in load resistance

In buck mode of operation, where I^*=30 A, I_2=30±0.5 A, V_2 = 170±1 V and load resistance changes from 2Ω to 1Ω. Initially here also, the load current I_2 and load voltage V_2 takes around 3ms to reach steady state value. The inductor current i_L is averaged at 29.42 A. A simulation result is shown in Fig.9. With change in load resistance, the inductor current i_L, load current increases immediately and i_L is feed back to regulator. Before the I_2 higher further, the regulator controls the load current to 30±1 A and load voltage decreases smoothly from 170±1 V to 140±01 V. The inductor current averaged at 29.19 A. Both load voltage and load current takes around 1ms to reach their steady state value.

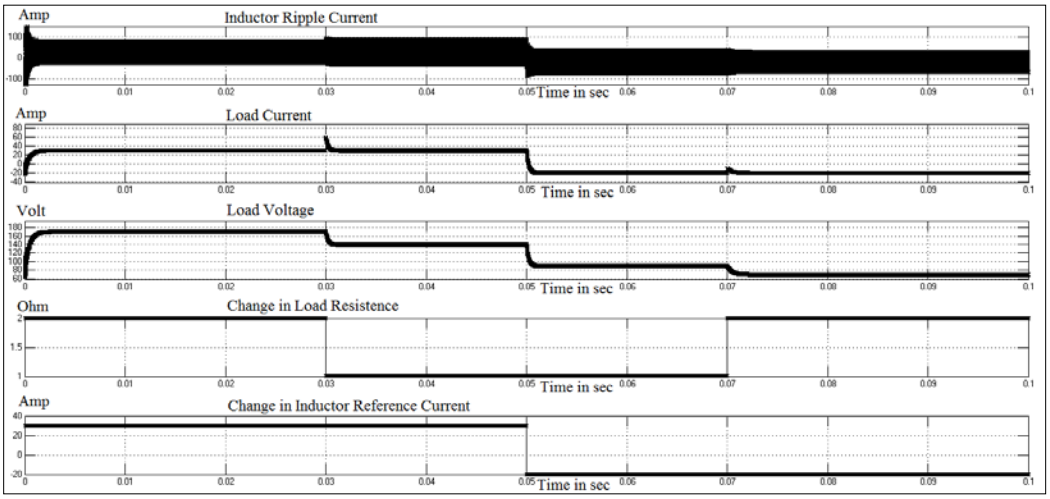

Fig.9 Simulation results for change in load resistance.

In boost mode of operation, where I^*=-20 A, I_2=-20±1 A, V_2 = 90±1 V and load resistance changes from 1Ω to 2Ω. Inductor current is averaged at -19.60 A. A simulation result is shown in same Fig .9. With change in load resistance, i_L decreases, I_2 increases immediately and i_L is given back to controller. Before I_2 increases further, the regulator regulates the I_2 back to its steady and V_2 decreases smoothly from 90±1 V to 70±01 V within 1.5ms. The inductor current is averaged at -19.46 A. The duty cycle changes smoothly during change in mode of operation and during change in load resistance as shown in Fig. 10. Variation of efficiency at different levels of load resistance is shown in Fig 11.

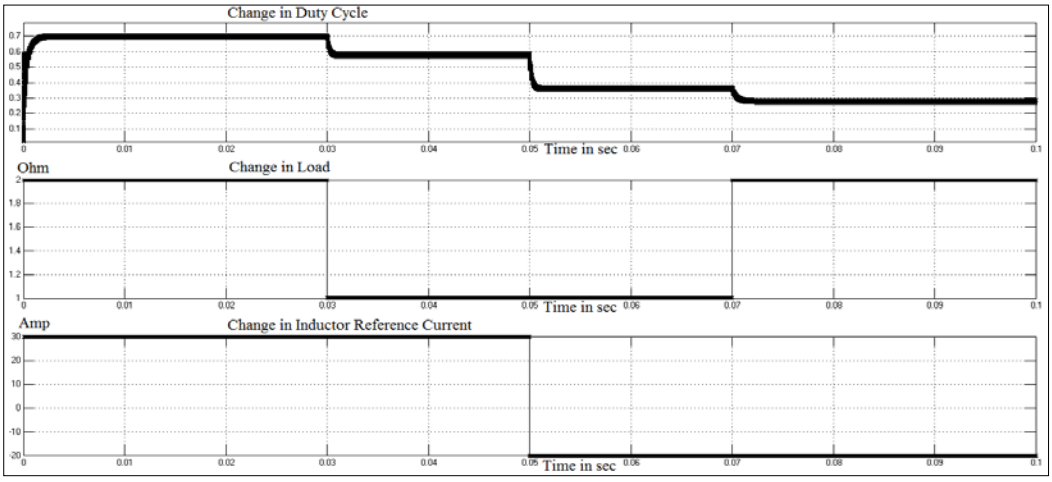

Fig.10 Simulation results of duty cycle for change in load resistance and for change in inductor reference current.

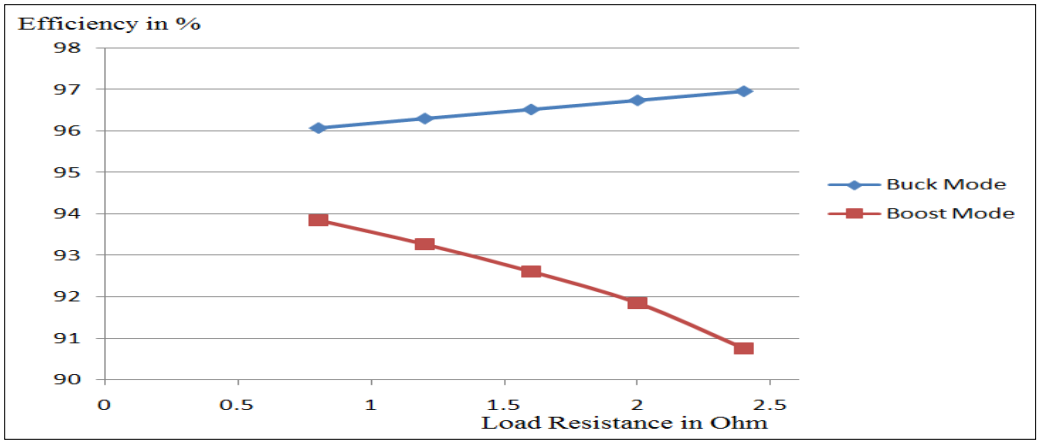

Fig.11 Load resistance v/s Efficiency.

Case 3: Change in input voltage

In buck mode of operation, where I*=30 A, I_2=30±0.5 A, V_2 = 170±1 V and input voltage changes from 260 V to 250 V. Initially, the load current I_2 and load voltage V_2 takes around 3ms to reach steady state value. A simulation result is shown in Fig. 12. The inductor average current is regulated at 29.44 A. With change in input voltage, the inductor current i_L, the load current I_2, load voltage V_2 depresses immediately and i_L is feed back to regulator. Before I_2 and V_2 reduce further, the regulator controls the load current and load voltage back to its steady state within 1.5ms. The averaged inductor current is 29.42 A.

In boost mode of operation, where I*=-20 A, I_2=-20±0.5 A, V_2 = 70±1 V and input voltage changes from 250 V to 260 V. The inductor current averaged at -19.47 A. A simulation result is shown in same Fig. 12. With change in input voltage, I_2, i_L, V_2 increases immediately and i_L is given back to regulator. Before I_2 and V_2 raises further, the regulator controls the load current and load voltage back to its steady state within 1.5ms. The averaged inductor current is -19.44 A. Duty cycle changes smoothly for change in mode of operation and for change in input voltage as shown in Fig. 13. Variation of efficiency at different levels of input voltage is shown in Fig. 14.

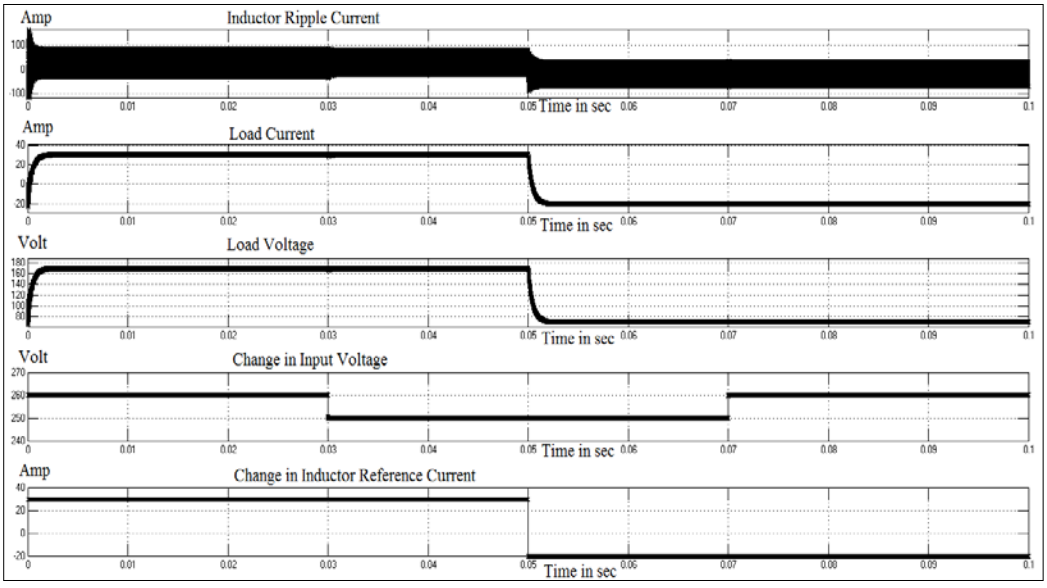

Fig.12 Simulation results for change in input voltage.

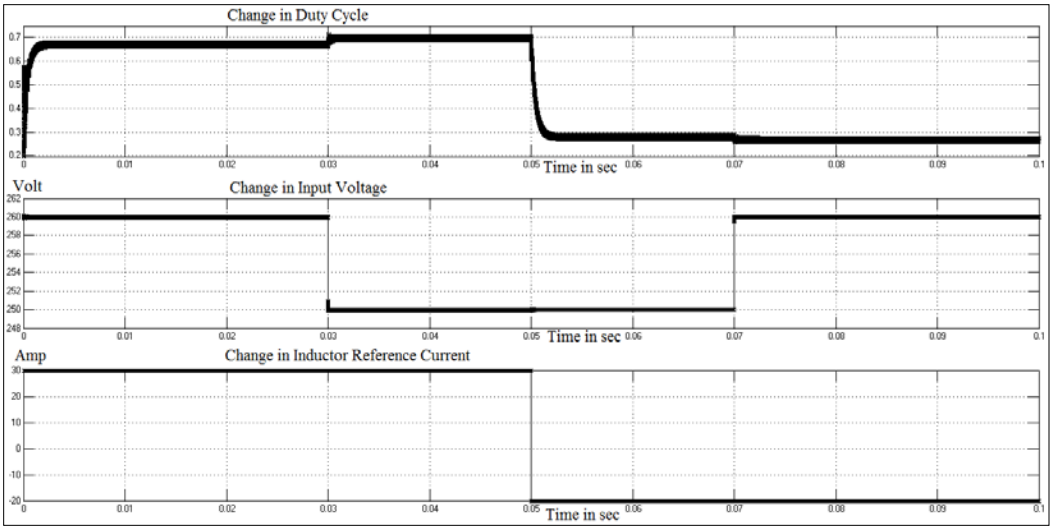

Fig.13 Simulation results of duty cycle for change in input voltage and for change in inductor reference current.

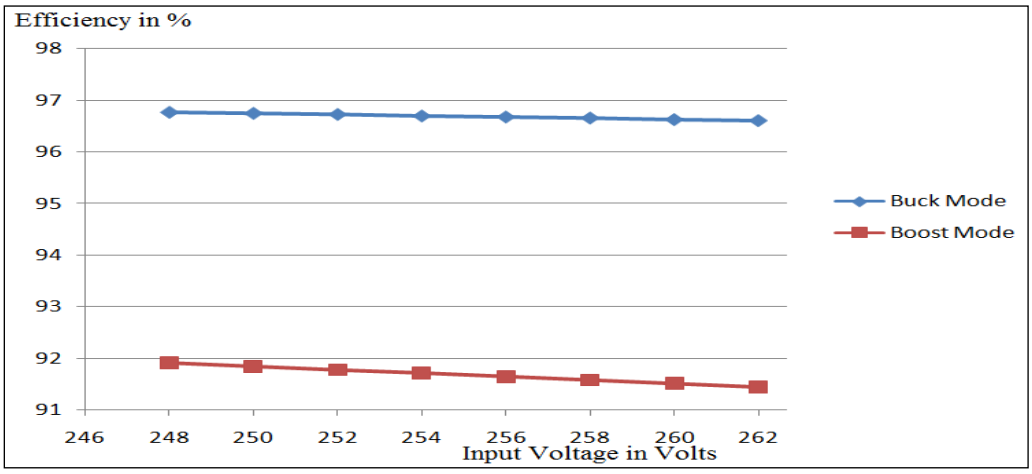

Fig.14 Input Voltage v/s Efficiency.

The theoretical and simulation measurements of different parameters for above three cases are tabulated in Table 4, 5 and 6 respectively and they are comparable. Efficiency variation, for switching frequency range from 10 kHz to 200 kHz, for three different test cases as given in Table 7, is shown in Fig 15. From the results obtained it is noted that, the efficiency is high in the range of 40 to 50 kHz. This frequency range is declared as optimal switching frequency.

TABLE 4 MEASURED TEST PARAMETERS FOR CHANGE IN INDUCTOR REFERENCE CURRENT.

Parameters	***I***= 30 A, R_L=2Ω, V_1≈ 250 V* **Buck Mode of Operation**		***I*** = -20 A, R_L=2Ω, V_1≈ 250 V* **Boot Mode of Operation**	
	Theoretical	**Simulation**	**Theoretical**	**Simulation**
V_2 [V]	170	170±1	70	70±1
$I_2 = \frac{V_2}{R_2}$ [A]	30	30±0.5	-20	-20±0.5
$P_o = I_2.V_2$ [kW]	5.1	5.1	-1.4	-1.4
I_{peak} [A]	84.30	83.08	30.40	30.44
I_{min} [A]	-24.30	-24.23	-70.40	-69.40
I_L [A]	30	29.42	-20	-19.48
ΔI_L [A]	54.30	54.16	50.40	50.41
η [%]	96.75	96.78	91.85	91.91
D [%]	68.91	70±1	27.43	27±1

TABLE 5 MEASURED TEST PARAMETERS FOR CHANGE IN LOAD RESISTANCE.

Parameters	Buck Mode of Operation, I*=30 A, V1≈ 250 V				Boost Mode of Operation, I*= -20 A, V1≈ 250 V			
	R_L = 2Ω		R_L = 1Ω		R_L = 1Ω		R_L = 2Ω	
	Theoretical	Simulation	Theoretical	Simulation	Theoretical	Simulation	Theoretical	Simulation
V_2 [V]	170	170±1	140	140±1	90	90±1	70	70±1
$I_2 = \frac{V_2}{R_2}$ [A]	30	30±0.5	30	30±1	-20	-20±1	-20	-20±0.5
$P_o = I_2.V_2$ [kW]	5.1	5.1	4.2	4.2	-1.8	-1.8	-1.4	-1.4
I_{peak} [A]	84.30	83.07	91.54	90.09	37.60	37.77	30.40	30.44
I_{min} [A]	-24.30	-24.22	-31.54	-31.71	-77.60	-76.97	-70.40	-69.37
I_L [A]	30	29.42	30	29.19	-20	-19.60	-20	-19.46
ΔI_L [A]	54.30	54.16	61.54	61.44	57.60	57.62	50.40	50.41
η [%]	96.75	96.78	96.19	96.21	93.57	93.58	91.85	91.89
D [%]	68.91	69.5±1	56.89	57.5±1	35.42	36±1	27.43	27.6±1

TABLE 6 MEASURED TEST PARAMETERS FOR CHANGE IN INPUT VOLTAGE.

Parameters	Buck Mode of Operation, I*=30 A, R_L=2Ω				Boost Mode of Operation, I*= -20 A, R_L=2Ω			
	V_{in}=260 V		V_{in}=250 V		V_{in}=250 V		V_{in}=260 V	
	Theoretical	Simulation	Theoretical	Simulation	Theoretical	Simulation	Theoretical	Simulation
V_2 [V]	170	170±1	170	170±1	70	70±1	70	70±1
$I_2 = \frac{V_2}{R_2}$ [A]	30	30±0.5	30	30±0.5	-20	-20±0.5	-20	-20±0.5
$P_o = I_2.V_2$ [kW]	5.1	5.1	5.1	5.1	-1.4	- 1.4	-1.4	-1.4
I_{peak} [A]	88.76	87.67	84.30	83.06	30.40	30.44	31.15	31.19
I_{min} [A]	-28.76	-28.78	-24.30	-24.22	-70.40	-69.38	-71.15	-70.07
I_L [A]	30	29.44	30	29.42	-20	-19.47	-20	-19.44
ΔI_L [A]	58.76	58.71	54.30	54.26	50.40	50.41	51.15	51.16
η [%]	96.63	96.65	96.75	96.78	91.85	91.89	91.51	91.56
D [%]	66.25	67.2±1	68.91	69.7±1	27.43	27.6±1	26.37	26.6±1

TABLE 7 DUPLEX MODE TEST CASE PARAMETERS FOR OPTIMAL SWITCHING FREQUENCY FINDING.

Mode	Case	V_H [V]	V_L [V]	R_1 [mΩ]	R_2 [Ω]	I^* [A]	P_o [KW]
Buck	1	250	110	10	2	30	5.1
	2	250	110	10	1	30	4.2
	3	260	110	10	2	30	5.1
Boost	1	250	110	10	2	-20	-1.4
	2	250	110	10	1	-20	-1.8
	3	260	110	10	2	-20	-1.4

VIII. CONCLUSION

A high-efficiency non-isolated synchronous bidirectional DC-DC switching power converter operating in SDCM of operation and feedback controller technique is proposed in this paper. The transfer function module is derived and it is used to tune the PID gain using PID tuner available in MATLAB simulink control design block.

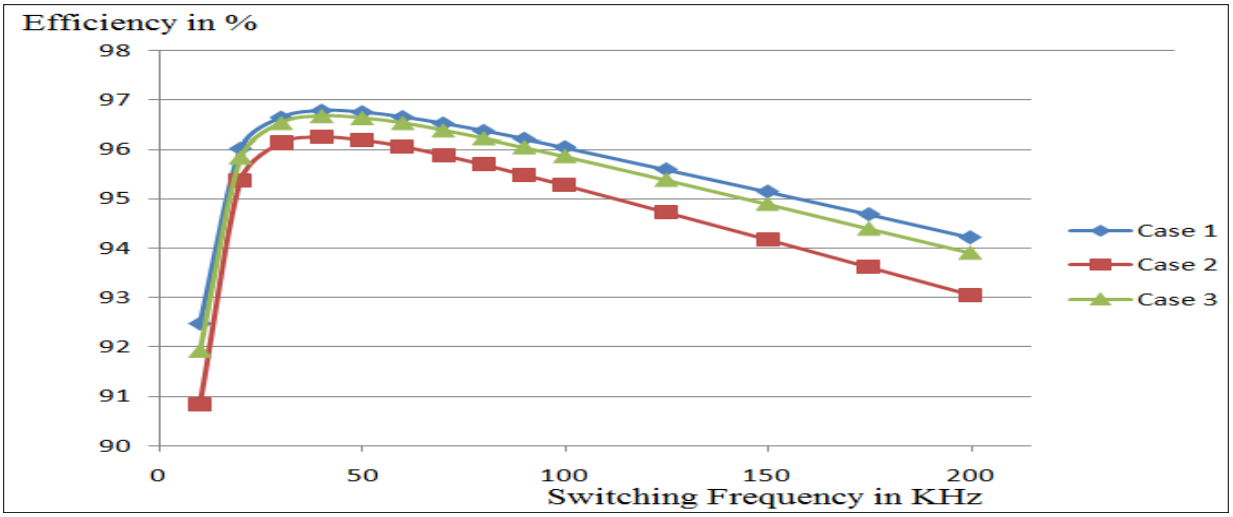

(a)

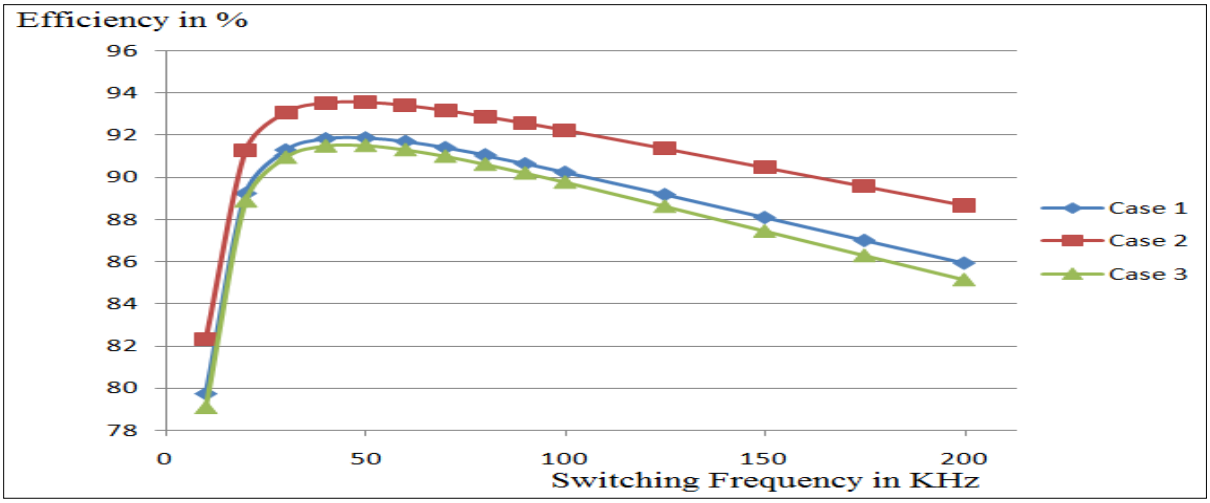

(b)

Fig.15 switching frequency v/s Efficiency for duplex mode of operation (a) buck mode (b) boost mode.

The controller works as expected and the system feature can be predicted through simulation. In all the above three cases it is noticed the duty cycle changes smoothly without severe change, this leads to smooth current and voltage flow, which minimize the stress in device. The time taken by load current and load voltage to reach steady state value for change in inductor reference current, change in load resistance and change in input voltage is around 1 to 2ms. The simulation efficiency in the range of 91.56% to 96.78% in different test conditions. The optimal switching frequency lies in the range of 40 to 50 KHz.

REFERENCES

[1] Jih-Sheng Lai and D. J. Nelson, "Energy management power converters in hybrid electric and fuel cell vehicles," in Proceedings of IEEE, Industrial Electron, Taipei, Taiwan, Vol. 95, Issue 4, pp. 766 – 777, April 2007.

[2] Premananda Pany, R.K. Singh and R.K. Tripathi, "Bidirectional DC-DC converter fed drive for electric vehicle system", International Journal of Engineering, Science and Technology, Vol. 3, No. 3, pp. 101-110, 2011.

[3] S.Dhanasekaran, E.Sowdesh Kumar and R.Vijaybalaji, "Different Methods of Control Mode in Switch Mode Power Supply- A Comparison", International Journal of Advanced Research in Electrical, Electronics and Instrumentation Engineering, Vol. 3, Issue 1, pp. 6717-6724, January 2014.

[4] Husain Ahmed and Dr. Abha Rajoriya, "Performance Assessment of Tuning Methods for PID Controller Parameter used for Position Control of DC Motor" , International Journal of u-and e-Service, Science and Technology, Vol.7, No.5, pp.139-150 , 2014.

[5] Kiam Heong Ang, Gregory Chong, and Yun Li, "PID Control System Analysis, Design, and Technology", IEEE Transactions on control systems technology, Vol. 13, No. 4, pp. 559-576, July 2005.

[6] Mohammad Reza Modabbernia et al, "The State Space Average Model of Buck- Boost Switching Regulator Including all of The System Uncertainties", International Journal on Computer Science and Engineering (IJCSE) , Vol. 5, No. 02, pp. 120-132, Feb 2013.

[7] R.Sudha and Mr.P.M Dhanasekaran, "DC-DC Converters Using PID Controller and Pulse Width Modulation Technique", International Journal of Engineering Trends and Technology (IJETT) – Vol. 7, No. 4, pp. 164-168, Jan 2014.

[8] H. Guldemir, "Modeling and Sliding Mode Control of Dc-Dc Buck-Boost Converter", 6th International Advanced Technologies Symposium (IATS'11), pp 475-480, 16-18 May 2011.

[9] K. Manickavasagam, "Fuzzy Logic Controller Based Signal Buck Boost Converter for Solar PV Cell", International Journal of Applied Power Engineering (IJAPE), Vol.3, No.1, pp. 1-8, April 2014.